

Studies in Numerical Nonlinear Instability. II. A New Look at $u_t + uu_x = 0$

F. VADILLO

*Departamento de Matematica Aplicada,
Facultad de Ciencias, Universidad del Pais Vasco, Bilbao, Spain*

AND

J. M. SANZ-SERNA

*Departamento de Ecuaciones Funcionales,
Facultad de Ciencias, Universidad de Valladolid, Valladolid, Spain*

Received July 24, 1985; revised January 15, 1986

It is shown that, in general leap-frog schemes, any particular unstable solution behaves as an attractor of other solutions. For a leap-frog discretization of $u_t + uu_x = 0$, a particular kind of unstable solution is constructed which generically attracts any other solution. Estimates of the overflow time are presented and related to the notions of stability threshold and restricted stability. © 1986 Academic Press, Inc.

1. INTRODUCTION

In his important paper [3], Fornberg studied the nonlinear instabilities of Crank–Nicolson and leap-frog discretizations of $u_t + uu_x = 0$. His work consists of the explicit construction of a *particular* initial perturbation of the trivial solution that quickly leads to machine overflow. In a *linear* problem the most general solution can be obtained by superposition of particular solutions or modes. It follows that as the time increases any solution will be (generically) dominated by the fastest growing mode. However, in nonlinear situations (as those considered in this paper) the absence of a superposition principle renders the significance of *particular* rapidly growing solutions not so clear. One of our aims in the present paper is to show that, in the leap-frog case, particular perturbations play a more important role than one may at first suspect. Namely they determine the long time behaviour of the scheme in a way to be made precise later. The underlying mechanism is the “incompressible” character of leap-frog discretizations, which is crucial in gaining insight into this sort of schemes. To render the article self-contained we have included a brief section on this mechanism which has been discussed in [9] (see also [12] and [13]).

Our analysis also illustrates the so-called “*restricted stability*” generally associated with discretizations of nonlinear PDEs, i.e., as the mesh is refined, the scheme becomes more vulnerable to (nonlinear) instabilities. In this regard our findings throw light into the *theoretical* aspects of stability in nonlinear discretizations of PDEs [4]. (General theories on discretization methods have tended to be either ODE biased or linearly oriented.) Moreover, the behavioural study of leap-frog schemes carried out in this series of papers [9, 12, 13] might be of some *practical* significance in that a better understanding of the possible pathologies may lead to more effective ways of suppressing them.

Some very useful references on nonlinear instabilities are [1, 2, 5]. A more complete discussion of the literature can be seen in [15].

2. LEAP-FROG DISCRETIZATIONS

The leap-frog discretization of the d -dimensional system of differential equations

$$d\mathbf{U}/dt = \mathbf{F}(\mathbf{U}) \tag{2.1}$$

is given by

$$\mathbf{U}^{n+1} = \mathbf{U}^{n-1} + 2k\mathbf{F}(\mathbf{U}^n), \quad n = 1, 2, 3, \dots, \tag{2.2}$$

where k denotes the time-step. In the applications we are interested in, (2.1) is the result of discretizing in space a time-dependent PDE, but this fact plays no role at this stage. It is well known that, for fixed k , the sequence $\mathbf{U}^0, \mathbf{U}^1, \mathbf{U}^2, \dots$, may possess a qualitative behaviour completely different from the behaviour of the solutions of (2.1).

The recursion (2.2) can be rewritten in the form

$$\mathbf{U}^{2n} = \mathbf{U}^{2n-2} + 2k\mathbf{F}(\mathbf{U}^{2n-1}), \tag{2.3a}$$

$$\mathbf{U}^{2n+1} = \mathbf{U}^{2n-1} + 2k\mathbf{F}(\mathbf{U}^{2n}), \tag{2.3b}$$

$n = 1, 2, \dots$, where we have simply displayed two consecutive steps. With the notation $\mathbf{U}^{2n} = \mathbf{P}^n, \mathbf{U}^{2n+1} = \mathbf{Q}^n$, (2.3) becomes

$$\mathbf{P}^n = \mathbf{P}^{n-1} + 2k\mathbf{F}(\mathbf{Q}^{n-1}), \tag{2.4a}$$

$$\mathbf{Q}^n = \mathbf{Q}^{n-1} + 2k\mathbf{F}(\mathbf{P}^n), \tag{2.4b}$$

a recursion that can be regarded as a consistent one-step discretization, with step-length $2k$, of the system

$$d\mathbf{P}/dt = \mathbf{F}(\mathbf{Q}), \tag{2.5a}$$

$$d\mathbf{Q}/dt = \mathbf{F}(\mathbf{P}). \tag{2.5b}$$

It was shown in [9] that the $2d$ -dimensional system (2.5) (the so-called *augmented system* associated with (2.1)) provides, for each fixed k , a good description of the behaviour of the sequence of $2d$ -vectors $(\mathbf{P}^0, \mathbf{Q}^0), (\mathbf{P}^1, \mathbf{Q}^1), (\mathbf{P}^2, \mathbf{Q}^2), \dots$, i.e., of the sequence $(\mathbf{U}^0, \mathbf{U}^1), (\mathbf{U}^2, \mathbf{U}^3), (\mathbf{U}^4, \mathbf{U}^5), \dots$.

The augmented system (2.5) is always (i.e., regardless of the particular \mathbf{F}) “divergence free” [9] and therefore its solutions $(\mathbf{P}(t), \mathbf{Q}(t))$, when plotted in the $2d$ -dimensional (\mathbf{P}, \mathbf{Q}) -space, behave like streamlines of an incompressible, steady flow: they must become closer to each other in regions where the flow accelerates. In other words, a solution $(\mathbf{P}(t), \mathbf{Q}(t))$ of (2.5) along which $d\mathbf{P}/dt, d\mathbf{Q}/dt$ increase must attract neighbouring solutions.

Similarly the mapping which takes $(\mathbf{U}^{2n-2}, \mathbf{U}^{2n-1})$ into $(\mathbf{U}^{2n}, \mathbf{U}^{2n+1})$ preserves the volume in $2d$ -space [9] and by the same reasons as before it can be concluded that if we are able to exhibit explicitly a particular solution of (2.2) possessing a violent growth, then neighbouring starting vectors will originate a sequence which, as n increases, becomes closer and closer to the known unstable solution.

3. FORNBERG’S RESULTS

We consider the 1-periodic initial value problem

$$u_t + uu_x = 0, \quad -\infty < x < \infty, t \geq 0, \tag{3.1a}$$

$$u(x, 0) = u_0(x), \tag{3.1b}$$

$$u(x + 1, t) = u(x, t), \quad -\infty < x < \infty, t \geq 0, \tag{3.1c}$$

where $u_0(x)$ is a 1-periodic datum. The problem (3.1) is discretized in space by introducing a grid $x_j = jh, j = 0, 1, \dots, d - 1, h = 1/d, d$ an integer, and approximating $u(x_j, t)$ by $U_j(t), j = 0, 1, \dots, d - 1$, where $U_j(t)$ are the solutions of the following initial value problem

$$dU_j/dt + U_j(U_{j+1} - U_{j-1})/(2h) = 0, \quad j = 0, 1, \dots, d - 1, \tag{3.2a}$$

$$U_j(0) = u_0(x_j), \quad j = 0, 1, \dots, d - 1. \tag{3.2b}$$

In (3.2a) we take $U_d \equiv U_0, U_{-1} \equiv U_{d-1}$ to account for the periodicity. It should be mentioned that Fornberg treats the more general space discretization

$$\theta U_j(U_{j+1} - U_{j-1})/(2h) + (1 - \theta)(U_{j+1}^2 - U_{j-1}^2)/(4h)$$

with θ a parameter. In this paper, for the time being, we restrict our attention to the case $\theta = 1$, leading to (3.2a). Other values of θ are briefly considered in the final section.

The system (3.2a) can be rewritten in the compact form (2.1) by setting $\mathbf{U} =$

$(U_0, U_1, \dots, U_{d-1})^T$ and defining $\mathbf{F}(\mathbf{U})$ to be the vector-valued function whose j -th component, $j = 0, 1, \dots, d-1$, is given by

$$F_j(\mathbf{U}) = -U_j(U_{j+1} - U_{j-1})/(2h).$$

It is important to note that \mathbf{F} is homogeneous of degree 2, i.e.,

$$\mathbf{F}(\mu\mathbf{V}) = \mu^2\mathbf{F}(\mathbf{V}), \tag{3.3}$$

for each real number μ and d -dimensional vector \mathbf{V} . The system (3.2a) is now discretized in time, with a constant step-length k , by means of the leap-frog technique. This results in the fully discrete scheme (2.2) or

$$U_j^{n+1} = U_j^{n-1} - \lambda U_j^n (U_{j+1}^n - U_{j-1}^n), \quad 0 \leq j \leq d-1, n = 1, 2, \dots, \tag{3.4}$$

where λ denotes the mesh-ratio k/h . The scheme (2.2) or (3.4) is complemented by the initial conditions

$$U_j^0 = u_0(x_j), \quad 0 \leq j \leq d-1,$$

with Euler's rule

$$\mathbf{U}^1 = \mathbf{U}^0 + k\mathbf{F}(\mathbf{U}^0)$$

providing the missing starting level.

Fornberg considers in [3] the case $u_0 \equiv 0$, leading of course of the trivial solution $u \equiv 0$ (and also to $U_j^n \equiv 0$) and studies the effect on U_j^n of small perturbations

$$U_j^0 = \sigma_j$$

of the identically zero initial conditions. Note that $U_j^n \equiv 0$ corresponds to a neutrally stable equilibrium in a linearized analysis. Fornberg's main point consists of the observation that if \mathbf{V} is an eigenvector of \mathbf{F} with eigenvalue γ , i.e.,

$$\mathbf{F}(\mathbf{V}) = \gamma\mathbf{V}, \tag{3.5}$$

then it is possible to use separation of variables in the partial difference system (3.4). Namely (3.4) will possess solutions of the form $U_j^n = a_n V_j$, provided that the a_n satisfy

$$a_{n+1} - a_{n-1} = 2k\gamma a_n^2, \quad n = 1, 2, \dots \tag{3.6}$$

(This follows easily from (3.3), (3.5).) The recurrence (3.6) is the leap-frog discretization of the ODE

$$da/dt = \gamma a^2, \quad t \geq 0 \tag{3.7}$$

whose solutions $a(t) = 1/((1/a(0)) - \gamma t)$ blow up at the finite time $t_{\max} = (a(0)\gamma)^{-1}$,

provided that $a(0)\gamma > 0$. (A recurrence similar to (3.6) has been analyzed in detail in [14]. For further results on (3.6) see [15].) From these considerations, Fornberg concluded that if an eigenvector \mathbf{V} could be found with nonzero eigenvalue γ , then the initial perturbation $\sigma = a_0 \mathbf{V}$ would induce extremely large perturbations by the time $(a_0\gamma)^{-1}$. Here a_0 must be chosen to have the sign of γ . (In [9] one of the present authors proved that the overflow will also be reached if a_0 and γ possess different signs, via the dynamics of the augmented system. However, the blow up time is in this case significantly larger.)

Next Fornberg observed that when d is a multiple of 3 the vector \mathbf{V} with components $V_{3j} = 0, V_{3j+1} = \varepsilon, V_{3j+2} = -\varepsilon, j = 0, 1, \dots, [d/3]$ (square brackets denote integer part) is an eigenvector with corresponding eigenvalue $\varepsilon/(2h)$. Thus, the initial perturbation $\dots, \varepsilon, 0, \varepsilon, -\varepsilon, \dots$, with positive ε , leads to blow-up by the time $2h/\varepsilon$. Note that this time decreases as the size ε of the perturbation increases and that for a given value of ε tends to zero with the mesh-size h . This phenomenon is linked to the idea of *stability thresholds*, to be discussed later.

4. THE BUTTERFLY CONFIGURATION

It is easy to check that if l is an integer, then the vector \mathbf{V} with components $V_l = \varepsilon, V_{l+1} = -\varepsilon, V_j = 0, j \neq l, l+1$ is also an eigenvector associated with the eigenvalue $\varepsilon/(2h)$. Vectors of this form will be called butterfly configurations, by reasons that will become clear immediately. The following points should be emphasized:

- (i) Butterfly configurations, while analogous to Fornberg's pattern, were not considered in [3].
- (ii) While Fornberg's pattern is unique (up to the size of ε), there is a butterfly configuration for each choice of $l, 0 \leq l \leq d-1$.
- (iii) The existence of a butterfly configuration does not require that d be a multiple of 3.

It is convenient to express vectors $\mathbf{V} = (V_0, V_1, \dots, V_{d-1})^T$ (or the grid functions represented by them) by means of discrete Fourier series. Restricting for simplicity our attention to the case where d is odd, $d = 2M + 1$, we consider representations of the form

$$\sum_{\omega = -M}^M a(\omega) \exp(2\pi i \omega x), \tag{4.1}$$

where, as it is well known, the $2M + 1$ coefficients $a(\omega)$ can be uniquely determined by the requirement that for $x = x_j, j = 0, 1, \dots, d-1$, (4.1) takes the prescribed value V_j . If \mathbf{V} has real entries, then $|a(-\omega)| = |a(\omega)|, \omega = 0, 1, \dots, M$, which implies that, if (4.1) is represented as a histogram displaying $|a(\omega)|$ against the frequency ω , then the result is symmetric with respect to the line $\omega = 0$.

When V is a butterfly configuration the corresponding histogram takes the form shown in Fig. 1a, thus explaining our terminology. In this figure, $d=99$, $h=\frac{1}{99}$, but other values of d lead to the same overall appearance. Note that the choice of the integer l which governs the location of the two nonzero entries in V does not affect the histogram: a change in l induces a change in the phases of $a(\omega)$, $\omega=0, \pm 1, \pm 2, \dots$, without altering the corresponding amplitudes. In the numerical experiments reported later we have chosen to present the corresponding histograms (power spectra) rather than physical space graphs. This has the advantage of giving the same appearance to all the butterfly configurations regardless of the particular value of l . However, it should be mentioned that the attractions to be described later would of course be apparent also in physical space.

To illustrate the growth of the solution U_j^n , induced by a perturbation σ at time $t=0$, in the case where σ is a butterfly configuration, we conducted an experiment with $d=99$, $\lambda=1$, $\varepsilon=0.1$. After 24 time-steps of (3.4) the resulting vector U^{25} has a maximum norm of 10^{14} . The corresponding histogram is displayed in Fig. 1b and is identical to that in Fig. 1a, because, when U^0 is an eigenvector, U^n is simply a scalar multiple of U^0 and our plotting routine adjusts automatically the vertical scale.

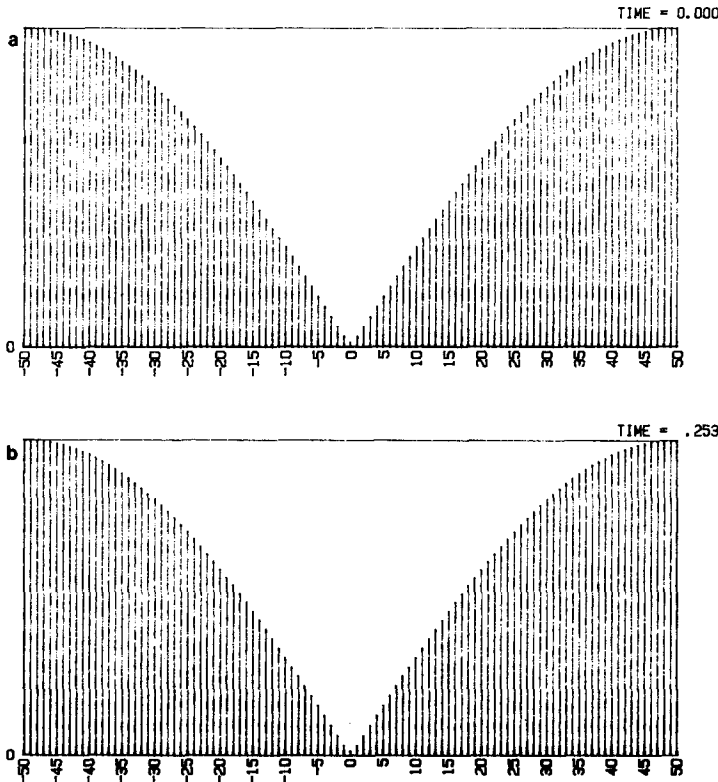


FIG. 1. Evolution of a butterfly initial perturbation.

Next, we show that, at least qualitatively, the growth in a butterfly configuration is the quickest possible among solutions of (3.4). We introduce the L_∞ and L_2 norms for vectors $\mathbf{V} = (V_0, V_1, \dots, V_{d-1})^T$ of grid values

$$\begin{aligned} \|\mathbf{V}\|_\infty &= \max_j |V_j|, \\ \|\mathbf{V}\|_2 &= \left(h \sum_{j=0}^{d-1} V_j^2 \right)^{1/2}. \end{aligned}$$

If \mathbf{U}^n , $n = 0, 1, 2, \dots$, is a solution of (3.4) we define the energies $E_n = \|\mathbf{U}^n\|_2$. On multiplying (3.4) by $U_j^{n+1} + U_j^{n-1}$ and adding, we easily obtain

$$\begin{aligned} |E_{n+1}^2 - E_{n-1}^2| &\leq \lambda h \sum_{j=0}^{d-1} |U_j^n| |U_{j+1}^n - U_{j-1}^n| |U_j^{n+1} + U_j^{n-1}| \\ &\leq \lambda h (\|\mathbf{U}^{n+1}\|_\infty + \|\mathbf{U}^{n-1}\|_\infty) \sum_{j=0}^{d-1} |U_j^n| (|U_{j+1}^n| + |U_{j-1}^n|) \\ &\leq \lambda (\|\mathbf{U}^{n+1}\|_\infty + \|\mathbf{U}^{n-1}\|_\infty) 2E_n^2. \end{aligned}$$

In the last step we have employed the Cauchy-Schwartz inequality and noted that the vectors $(U_1^n, U_2^n, \dots, U_{d-1}^n, U_0^n)^T$ and $(U_{d-1}^n, U_0^n, \dots, U_{d-2}^n)^T$ have both L_2 norm E_n . On invoking the relation $\|\mathbf{V}\|_\infty \leq h^{-1/2} \|\mathbf{V}\|_2$, which links the L_∞ and L_2 norms, we finally arrive at the difference inequality

$$E_{n+1}^2 \leq E_{n-1}^2 + 2\lambda h^{-1/2} E_n^2 (E_{n+1} + E_{n-1}),$$

or

$$E_{n+1} \leq E_{n-1} + 2\lambda h^{-1/2} E_n^2 \tag{4.2}$$

for the growth in energy of the solutions of (3.4).

For a butterfly configuration, $U_j^n = 0$ if $j \neq l, l+1$ and $U_{l+1}^n = -U_l^n < 0$. Therefore $E_n = (2h)^{1/2} U_l^n$ or $U_l^n = (2h)^{-1/2} E_n$. Substitution in (3.4) leads to

$$E_{n+1} = E_{n-1} + 2^{-1/2} \lambda h^{-1/2} E_n^2. \tag{4.3}$$

Thus the recursion (4.3) governing the energy growth for butterfly configurations is identical, except for a constant factor $2\sqrt{2}$, to the recursion (4.2) which sets an upper bound on the growth of *any* solution of (3.4). Therefore the discussion in Section 2 suggests that butterfly configurations may act as attractors of solutions of (3.4), i.e., for large values of n , \mathbf{U}^n is likely to be close to a butterfly even if \mathbf{U}^0 is not.

Note that (4.3) can be viewed as the leap-frog discretization of the ODE

$$dE/dt = (2h)^{-3/2} E^2,$$

with solutions

$$E(t) = 1/(E(0)^{-1} - (2h)^{-3/2}t),$$

which become infinite at $t_{\max} = (2h)^{3/2}/E(0)$ if $E(0) > 0$. Of importance here is the fact that the growths involved are essentially more violent than the exponential growths which can be found in linear problems.

For (4.2) a similar analysis is possible and leads to $t_{\max} = h^{3/2}/E(0)$. On the other hand for Fornberg's pattern one would find $t_{\max} = 2^{3/2}3^{-1/2}h/E(0)$, showing an $O(h)$ dependence on h rather than the $O(h^{3/2})$ behaviours found for the general and butterfly solutions.

In a linear problem, the Lax stability requirement [8, 6, 7, 11, 10]

$$\|U^n - V^n\| \leq C \|U^0 - V^0\|, \quad 0 \leq nk \leq T < \infty, k \leq k_0, \quad (4.4)$$

where U^n, V^n are two solutions of the difference scheme and C is independent of U^n, V^n and the mesh sizes, guarantees the convergence of consistent discretizations for $0 \leq t \leq T$, and is even necessary for such convergence when this is asked for all initial data in a Banach space. It is clear that in the present nonlinear scheme (4.4) cannot be valid. (Set $V^n \equiv 0$ and U^n originating from a butterfly configuration, fix $E(0)$ and let $h \rightarrow 0$. Then the left-hand side blows up.)

In order that (4.4) holds for $V^n \equiv 0$, one should only allow perturbations for which $\|U^0\| = o(h^{3/2})$, so that the corresponding blow up time occurs for $t_{\max} > T$. This sort of behaviour, where there is a *threshold* on the size of the allowable perturbations which decreases with h and k was called by Stetter *restricted stability* and is compatible with convergence for smooth solutions. A long discussion on this point, along with a list of relevant references are given in [4].

5. NUMERICAL EXPERIMENTS

The scheme was run on a computer for a large choice of values of h and initial perturbations $\sigma_j, j = 0, 1, \dots, d-1$, while keeping $\lambda = 1$. This represents no restriction of the generality since, with h and σ varying, λ can be scaled out by a change in the units for U . Hundreds of experiments were conducted and only a small representative selection can be reported here. Three alternative techniques were used to generate the vector of perturbations σ . They will be discussed successively.

(i) Localized Perturbations

Here $\sigma_j = 0$ except for $j = 0, 1, \dots, r$ with r a small integer. Examples include

- (A) $\sigma_0 = \sigma_1 = \sigma_2 = \varepsilon > 0; \sigma_j = 0$ if $j > 2$.
- (B) $\sigma_j = \varepsilon > 0$, if $0 \leq j \leq 8; \sigma_j = 0$ if $j > 8$.
- (C) $\sigma_0 = \sigma_2 = \varepsilon > 0, \sigma_1 = -\varepsilon; \sigma_j = 0$ if $j > 2$.
- (D) $\sigma_0 = \sigma_1 = \varepsilon > 0, \sigma_2 = -\varepsilon; \sigma_j = 0$ if $j > 2$.
- (E) $\sigma_0 = \varepsilon > 0, \sigma_1 = 0, \sigma_2 = -\varepsilon; \sigma_j = 0$ if $j > 2$.

TABLE I
Localized Perturbations

| σ | $\ \sigma\ _\infty$ | $\ \sigma\ _2$ | Location of overflow |
|-----------|---------------------|----------------|----------------------|
| Butterfly | 0.1 | 0.0142 | 29 |
| A | 0.1 | 0.0174 | 172 |
| B | 0.1 | 0.0302 | 264 |
| C | 0.1 | 0.0174 | 27 |
| D | 0.1 | 0.0174 | 27 |

The initial configuration (E) is an eigenvector with zero eigenvalue and behaved in a stable manner. The initial perturbations (A)–(D) lead to machine overflow. (The computer employed can represent number up to 10^{499} . Since the L_2 norm of the solution was computed at each step and this involves squaring the entries, overflow means that a value of U_j^n was found which exceeded the square root of 10^{499} .) The

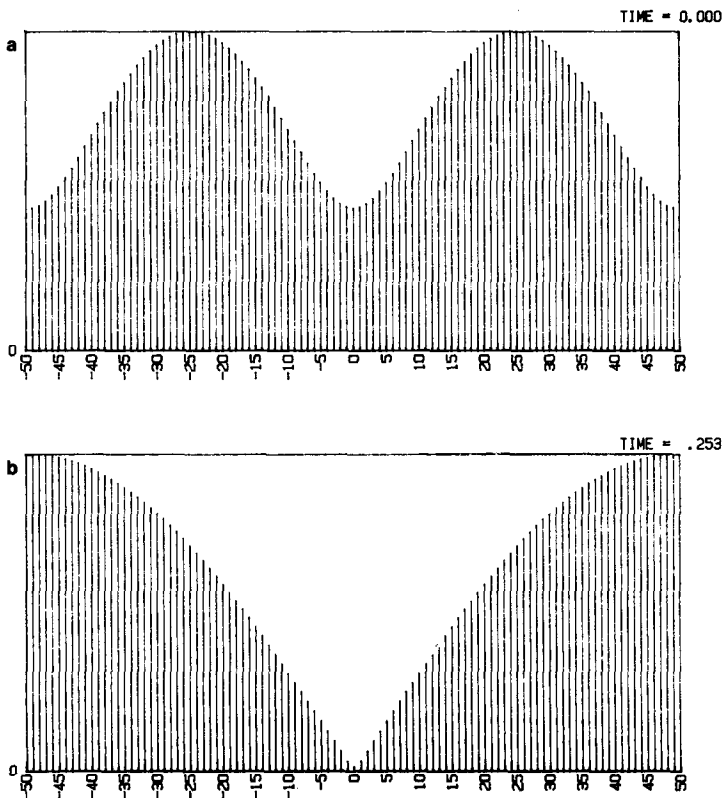


FIG. 2. Evolution of a localized (D) initial perturbation.

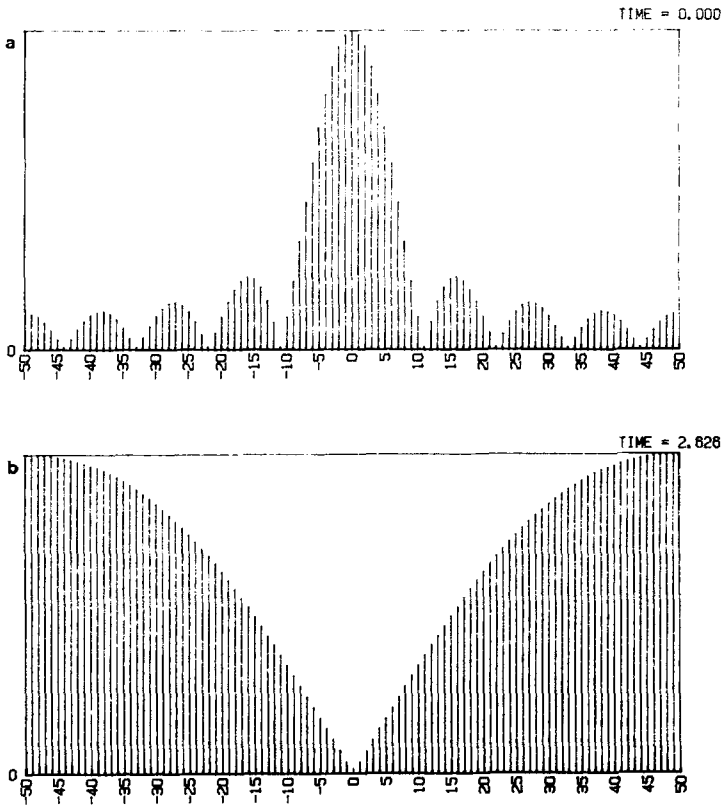


FIG. 3. Evolution of a localized (B) initial perturbation.

Table I provides the value of n for which the overflow took place when $\varepsilon = 0.1$, $h = 1/99$; the corresponding butterfly run has also been included for comparison. In all the runs, regardless of the initial choice of σ , we observed that, in the time-steps preceding the blow up, U^n was very close to a butterfly configuration. This is illustrated in Fig. 2, which corresponds to the initial perturbation (D) with $\varepsilon = 0.1$, $h = \frac{1}{99}$. The plot (a) depicts the initial condition ($n = 0$), while (b) corresponds to

TABLE II
Random Perturbations

| σ | $\ \sigma\ _{\infty}$ | $\ \sigma\ _2$ | Location of overflow |
|-----------|-----------------------|----------------|----------------------|
| Butterfly | 0.1 | 0.0142 | 29 |
| Seed 444 | 0.2444 | 0.1372 | 60 |
| Seed 4500 | 0.2488 | 0.1331 | 55 |

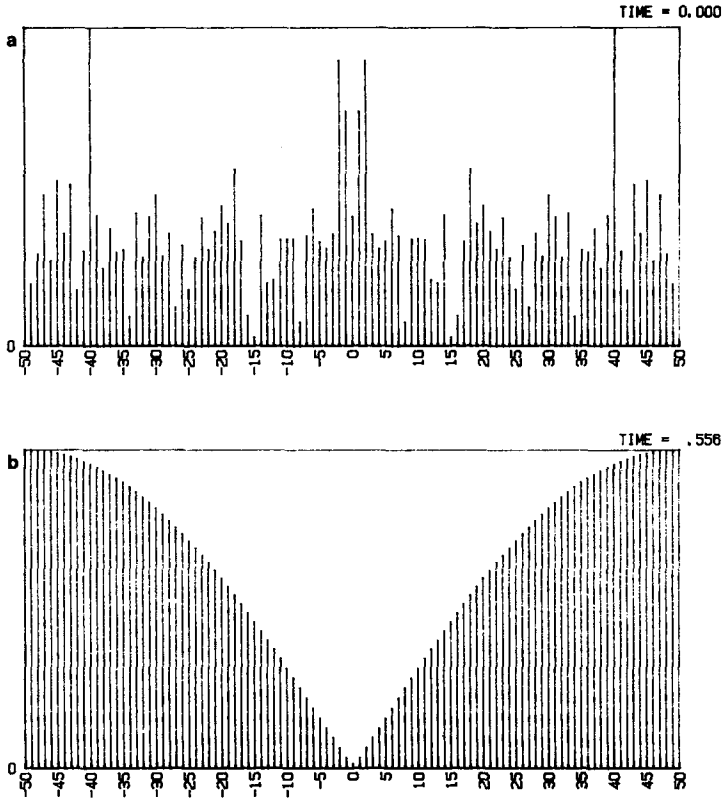


FIG. 4. Evolution of a random initial perturbation.

$n = 25$, when $\|U^n\|_2 \simeq 10^{100}$. Figure 3 refers to the perturbation (B), with $\varepsilon = 0.1$, $h = \frac{1}{99}$, $n = 0$, $n = 260$, $\|U^{260}\| \simeq 10^{31}$.

(ii) *Random Perturbations*

Now $\sigma_j, j = 0, 1, \dots, d - 1$, were formed by d consecutive calls to the random number generator of the computer, starting with an arbitrarily chosen "seed." The numbers returned by the random number subroutine have a uniform distribution in $[-1, 1]$ and are subsequently scaled to an interval $[-\eta, \eta]$. For $h = \frac{1}{99}$, 25 seeds were tried with different choices of the scaling parameter η . We found that the occurrence or otherwise of a blow-up before a given time was dependent on η but fairly independent of the choice of seed. Table II corresponds to $\eta = 0.25$ and two different seeds.

Again it was observed that the initial perturbation invariably evolved into a butterfly configuration. In Fig. 4, $\eta = 0.05$. The random aspect at $n = 0$ has given rise to a butterfly configuration by $n = 55$, $\|U^{55}\| \simeq 10^{18}$.

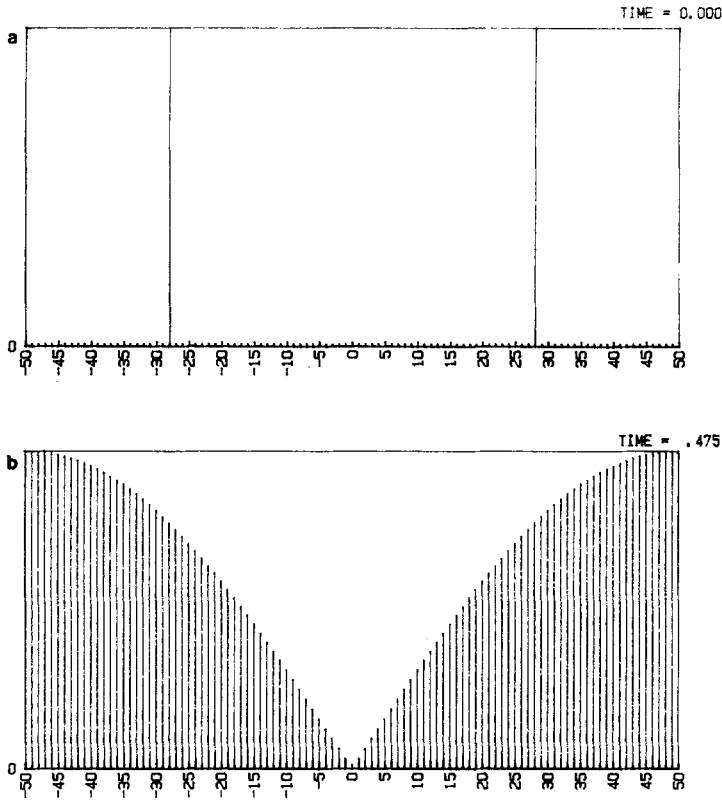


FIG. 5. Evolution of a single frequency initial perturbation.

(iii) *Systematic Perturbations*

These corresponds to initial perturbations with a single frequency

$$\sigma_j = A \sin 2\pi\mu x_j + B \cos 2\pi\mu x_j.$$

In Fig. 5 we have followed the evolution of the case $A = B = 0.04$, with initial L_2 norm 0.05656 and overflow at $n = 50$. (Compare this value with $n = 29$ for the butterfly configuration with the much smaller norm 0.0142.) The plot (b) corresponds to $n = 47$ with $\|U^{47}\| \simeq 10^{78}$. The choice of frequency μ is not crucial. Table III has also $h = \frac{1}{99}$ and six different frequencies. The attraction towards a butterfly configuration was detected in all the experiments in this group.

Experiments were also satisfactorily conducted which tested the $h^{3/2}$ threshold behaviour and our estimates of the blow-up time. The interested reader is once more directed to the thesis [15].

TABLE III
One Frequency Perturbation
Location of Overflow

| μ | $A = B = 1$ | $A = 1, B = 0$ | $A = 0, B = 1$ |
|-------|-------------|----------------|----------------|
| 8 | 12 | 13 | 13 |
| 25 | 11 | 12 | 12 |
| 33 | 12 | 12 | 12 |
| 44 | 12 | 14 | 13 |
| 60 | 11 | 12 | 12 |
| 72 | 11 | 12 | 12 |

6. CONCLUDING REMARKS

For a leap-frog discretization of $u_t + uu_x = 0$, a particular initial perturbation, the butterfly configuration, has been constructed which quickly leads to machine overflow. The blow-up time has been estimated. Due to the incompressible character of leap-frog schemes, these particular perturbations must attract neighbouring solutions. In fact, it has been shown experimentally that butterfly configurations attract any other solution generically (i.e., except for some trivial counterexamples).

In general nonlinear discretizations, it is by no means true that the fastest growing solution attracts the remaining solutions. One of our purposes in this paper has been to show that that is, however, the case for leap-frog schemes, due to the incompressibility-conservation of volume property. While in the present article we have chosen the scheme (3.4) as a case study, it is clear that the underlying mechanism is present in all leap-frog schemes. Our choice of (3.4) as test discretization was not of course dictated by its practical value (which is very small: bad stability properties and lack of convergence in the presence of shocks) but rather by its amenability to the analysis.

In [15] other values of the parameter θ which governs the space discretization of (3.1a) have been considered, $0 \leq \theta \leq 1$. For all of these, including $\theta = \frac{1}{3}$ for which the semidiscrete scheme conserves the L^2 norm, the basic phenomenon studied in this paper was found to apply, namely, as t increases, generic solutions are attracted towards well-identified patterns in Fourier space associated with violent growths. The shape of the power spectrum of the attractor and the blow-up time depend on θ , as one may expect. Not surprisingly the blow-up time is largest for $\theta = \frac{1}{3}$. It was not always possible to describe analytically the attracting pattern and this precluded an investigation of the energy growth similar to that given here for $\theta = 1$.

REFERENCES

1. H. AREF AND P. K. DARIPA, *SIAM J. Sci. Stat. Comput.* **5**, 856 (1984).
2. W. L. BRIGGS, A. C. NEWELL AND T. SARIE, *J. Comput. Phys.* **51**, 83 (1983).

3. B. FORNBERG, *Math. Comput.* **27**, 45 (1973).
4. J. C. LÓPEZ-MARCOS AND J. M. SANZ-SERNA, *IMA J. Numer. Anal.*, in press.
5. A. MAJDA AND S. OSHER, *Numer. Math.* **30**, 429 (1978).
6. C. PALENCIA AND J. M. SANZ-SERNA, *IMA J. Numer. Anal.* **4**, 109 (1984).
7. C. PALENCIA AND J. M. SANZ-SERNA, *Numer. Math.* **44**, 279 (1984).
8. R. RICHTMYER AND K. W. MORTON, *Difference Methods for Initial Value Problems* (Wiley-Interscience, New York, 1967).
9. J. M. SANZ-SERNA, *SIAM J. Sci. Stat. Comput.* **6**, 923 (1985).
10. J. M. SANZ-SERNA, in *Nonlinear Differential Equations and Applications*, edited by J. K. Hale and P. Martinez-Amores (Pitman, London, 1985), p. 64.
11. J. M. SANZ-SERNA AND C. PALENCIA, *Math. Comput.* **45**, 143 (1985).
12. J. M. SANZ-SERNA AND F. VADILLO, in *Proceedings Dundee 1985*, edited by D. F. Griffiths and G. A. Watson (Pitman, London, in press).
13. J. M. SANZ-SERNA AND F. VADILLO, Studies in numerical nonlinear instability III: Augmented Hamiltonian systems, *SIAM J. Appl. Math.*, in press.
14. J. M. SANZ-SERNA AND J. VERWER, *J. Math. Anal. Appl.* **116**, 456 (1986).
15. F. VADILLO, Thesis, Valladolid, 1985 (unpublished).